The Plant Cell, Vol. 17, 2601–2613, September 2005, www.plantcell.org

Arabidopsis SENESCENCE-ASSOCIATED GENE101 Stabilizes and Signals within an ENHANCED DISEASE SUSCEPTIBILITY1 Complex in Plant Innate Immunity [W]

Bart J. Feys,[a,b,1] Marcel Wiermer,[c,1] Riyaz A. Bhat,[c] Lisa J. Moisan,[a] Nieves Medina-Escobar,[c,2] Christina Neu,[c] Adriana Cabral,[c,3] and Jane E. Parker[c,4]

[a] Sainsbury Laboratory, John Innes Centre, Norwich NR4 7UH, United Kingdom
[b] Department of Biological Sciences, Imperial College London, South Kensington Campus, London SW7 2AZ, United Kingdom
[c] Department of Plant–Microbe Interactions, Max-Planck-Institute for Plant Breeding Research, 50829 Cologne, Germany

Plant innate immunity against invasive biotrophic pathogens depends on the intracellular defense regulator ENHANCED DISEASE SUSCEPTIBILITY1 (EDS1). We show here that *Arabidopsis thaliana* EDS1 interacts in vivo with another protein, SENESCENCE-ASSOCIATED GENE101 (SAG101), discovered through a proteomic approach to identify new EDS1 pathway components. Together with PHYTOALEXIN-DEFICIENT4 (PAD4), a known EDS1 interactor, SAG101 contributes intrinsic and indispensable signaling activity to EDS1-dependent resistance. The combined activities of SAG101 and PAD4 are necessary for programmed cell death triggered by the Toll-Interleukin-1 Receptor type of nucleotide binding/leucine-rich repeat immune receptor in response to avirulent pathogen isolates and in restricting the growth of normally virulent pathogens. We further demonstrate by a combination of cell fractionation, coimmunoprecipitation, and fluorescence resonance energy transfer experiments the existence of an EDS1–SAG101 complex inside the nucleus that is molecularly and spatially distinct from EDS1–PAD4 associations in the nucleus and cytoplasm. By contrast, EDS1 homomeric interactions were detected in the cytoplasm but not inside the nucleus. These data, combined with evidence for coregulation between individual EDS1 complexes, suggest that dynamic interactions of EDS1 and its signaling partners in multiple cell compartments are important for plant defense signal relay.

INTRODUCTION

In plants, cellular innate immune responses are indispensable for defense against pathogens. *Arabidopsis thaliana ENHANCED DISEASE SUSCEPTIBILITY1* (*EDS1*) and *PHYTOALEXIN-DEFICIENT4* (*PAD4*) are essential regulators of basal resistance to invasive obligate biotrophic and certain hemibiotrophic pathogens, controlling defense amplification and the accumulation of the phenolic signaling molecule salicylic acid (Zhou et al., 1998; Jirage et al., 1999; Petersen et al., 2000; Feys et al., 2001). Also, EDS1 is necessary for *RESISTANCE* (*R*) gene–triggered programmed cell death conditioned by a type of intracellular nucleotide binding/leucine-rich repeat (NB-LRR) protein that has N-terminal homology (the Toll-Interleukin-1 Receptor [TIR] domain) with internal signaling domains of animal Toll-like receptors (Aarts et al., 1998; Feys et al., 2001). Generally, intracellular NB-LRR proteins possessing an N-terminal coiled-coil (CC) motif confer resistance and programmed cell death independently of EDS1, favoring the idea that EDS1 represents a point of signal discrimination between these two types of immune receptors (Aarts et al., 1998). This discrimination is not absolute, because at least one *Arabidopsis* CC-NB-LRR protein, HYPERSENSITIVE RESPONSE TO TURNIP CRINKLE VIRUS, which mediates viral resistance (Chandra-Shekara et al., 2004), and two CC proteins with a predicted transmembrane domain, RESISTANCE TO POWDERY MILDEW8 (RPW8.1) and RPW8.2, which confer fungal resistance (Xiao et al., 2003, 2005), also depend on EDS1 and PAD4. Further genetic analyses position EDS1 and PAD4 downstream of activated TIR-type NB-LRR proteins (Zhang et al., 2003; Zhou et al., 2004) and more pivotally as transducers of signals in redox stress (Rustérucci et al., 2001; Brodersen et al., 2002; Mateo et al., 2004). EDS1 and PAD4 have homology with eukaryotic lipases, and embedded in the conserved domains are three potential catalytic residues, a Ser, an Asp, and a His, that constitute an α/β hydrolase catalytic triad (Falk et al., 1999; Jirage et al., 1999), although no esterase activities have been demonstrated for these proteins. However, *EDS1* and *PAD4* share a domain of high sequence similarity (the EP domain) in their C termini with one other plant lipase-like sequence, *SENESCENCE-ASSOCIATED GENE101* (*SAG101*), that was identified previously as a senescence-associated gene

[1] These authors contributed equally to this work.
[2] Current address: Department of Molecular Biology and Biochemistry, University of Malaga, 29701 Malaga, Spain.
[3] Current address: Department of Molecular and Cellular Biology, University of Utrecht, 3584 CH Utrecht, The Netherlands.
[4] To whom correspondence should be addressed. E-mail parker@mpiz-koeln.mpg.de; fax 49-221-5062353.
The author responsible for distribution of materials integral to the findings presented in this article in accordance with the policy described in the Instructions for Authors (www.plantcell.org) is: Jane E. Parker (parker@mpiz-koeln.mpg.de).
[W] Online version contains Web-only data.
Article, publication date, and citation information can be found at www.plantcell.org/cgi/doi/10.1105/tpc.105.033910.

in *Arabidopsis* and that encodes a protein with apparent acyl hydrolase activity after expression in *Escherichia coli* (Feys et al., 2001; He and Gan, 2002).

Complete loss of TIR-NB-LRR conditioned resistance and its associated cell death program in *Arabidopsis eds1* mutants and partial disabling of the same resistance in *pad4* suggested a mechanism in which TIR-type NB-LRR proteins engage EDS1 early in the defense cascade that connects the recognition process to basal defenses, requiring both EDS1 and PAD4 (Feys et al., 2001). Consistent with such a cooperative role, EDS1 and PAD4 interacted in yeast two-hybrid assays and coimmunoprecipitated in *Arabidopsis* soluble leaf extracts (Feys et al., 2001). EDS1 could also form homomeric dimers in yeast. Here, we report the discovery of *Arabidopsis* SAG101 as an additional in vivo EDS1 partner and provide evidence that SAG101 and PAD4 together signal within the EDS1 disease resistance pathway. The combined results of cell fractionation, coimmunoprecipitation, and fluorescence resonance energy transfer (FRET) experiments reveal that different EDS1 complexes exist in the nucleus and cytoplasm.

RESULTS

SAG101 Is Part of an EDS1 Complex in Vivo

Previously, we identified PAD4 as an EDS1 interactor in a yeast two-hybrid screen and confirmed the presence of the EDS1–PAD4 complex in soluble leaf extracts by coimmunoprecipitation (Feys et al., 2001). To find additional in planta EDS1 interactors, we made stable transgenic lines of *eds1-1* (accession Wassilewskija [Ws-0]) and *eds1-2* (Landsberg *erecta* [L*er*]) null mutants expressing genomic *EDS1* driven by 1.4 kb of native promoter and containing, respectively, an N-terminal fusion of a single hemagglutinin (HA) epitope and a tandem affinity purification (TAP) tag (Rigaut et al., 1999). Multiple independent HA- and TAP-tagged EDS1 lines exhibited full restoration of wild-type resistance to avirulent isolates of the oomycete pathogen *Peronospora parasitica* in transgenic *eds1-1* and *eds1-2* lines (data not shown). A representative HA-EDS1 line expressing the fusion protein at levels comparable to those in the wild type (Figure 1A; data not shown) was chosen for affinity purification. Total soluble protein from unchallenged leaves of HA-EDS1 or control wild-type Ws-0 plants was incubated with anti-HA high-affinity antibody-coupled agarose beads, and proteins eluted from the beads were separated by SDS-PAGE (Figure 1B). Differential protein bands were excised and their identities determined by matrix-assisted laser-desorption ionization time of flight (MALDI-TOF) and quadrupole time of flight (Q-TOF) mass spectrometry. Eighteen tryptic peptides were derived from the SAG101 protein, representing total protein coverage of 40%. Of these, 12 peptides were subsequently unambiguously assigned by tandem mass spectrometry sequencing to SAG101 (Figure 1C; data not shown). One sequenced peptide was found to be Ws-0–specific, containing a single amino acid polymorphism (underlined: ILEIHNPPYSNQDPGLQVSK) compared with the SAG101 Columbia-0 (Col-0) reference sequence in the GenBank database used for mass spectrometry searches. Identification of this peptide reveals that the previously published *SAG101* mRNA sequence (He and Gan, 2002) misses the first 48 amino acids of the 537-amino acid SAG101 protein. A new start codon for SAG101 was confirmed by RT-PCR analysis of Col-0 RNA (data not shown) and matched an *Arabidopsis* Ws-0–derived EST (AY086301). The SAG101 protein sequence contains a putative signal peptide (cleavage after residue 27) and a potential nuclear localization signal (KKKK, amino acids 48 to 51) (Figure 1D). The predicted molecular mass of the SAG101 protein (62 kD) correlates with its electrophoretic mobility (Figure 1B). A sequence alignment of the N termini of EDS1, PAD4, and SAG101 shows an apparent lack of conservation in SAG101 of previously identified catalytic residues that potentially form part of a lipase/esterase catalytic triad (Figure 1D). Additionally, we identified SAG101 as an in planta EDS1 interactor using transgenic lines expressing TAP-tagged EDS1 (data not shown) and therefore were able to rule out artifacts associated with any particular affinity tag. These data show that EDS1 associates directly or indirectly with SAG101 in soluble extracts of healthy (pathogen-unchallenged) leaves. EDS1 was also identified by mass spectrometry analysis in fractions that eluted specifically from HA-tagged EDS1 transgenic material (Figure 1B; data not shown). PAD4-derived peptides were not detected in these experiments. An anti-PAD4 antiserum was not available to test whether low amounts of PAD4 purified with the EDS1 protein.

SAG101 Signals in Innate Immunity

To assess whether *SAG101* is necessary for plant defense, we isolated two independent lines from the Sainsbury Laboratory *Arabidopsis thaliana* transposants (SLAT) collection (Tissier et al., 1999) in accession Col-0 that were homozygous for dSpm transposon insertions within the *SAG101* gene (referred to as *sag101-1* and *sag101-2*). In both lines, the transposon had inserted within exonic sequences (Figure 2A). A rabbit polyclonal antiserum was raised to two unique SAG101 peptides. A band of the expected size of *Arabidopsis* SAG101 protein (~62 kD) that was undetectable in samples from *sag101-1* and *sag101-2* cross reacted with this antiserum on a protein gel blot of Col-0 soluble leaf extracts (Figure 2B), suggesting that both are null alleles.

The *sag101-1* and *sag101-2* mutants were tested for expression of race-specific resistance conferred by various TIR-NB-LRR–type *R* genes. After inoculation with avirulent *P. parasitica* isolate Cala2, *sag101-2* (Figure 3A) and *sag101-1* (data not shown) exhibited *RPP2*-triggered programmed cell death (hypersensitive response) at pathogen infection sites, and both mutants prevented pathogen sporulation on leaves as in the wild-type parental line, Col-0 (Figure 3B). This response was in contrast to that of the Col-0 *pad4-1* mutant, which has weakened *RPP2* resistance, manifested as trailing plant cell necrosis and significant pathogen sporulation (Figure 3B). Similar results were obtained when *sag101* and *pad4-1* mutants were tested for *RPP4* recognition of *P. parasitica* isolate Emwa1 (data not shown). We tested whether *SAG101* could be redundant with *PAD4* by making *pad4-1 sag101* double mutants. Leaves of *pad4-1 sag101* exhibited loss of *RPP2* resistance that was as extreme as the susceptibility of *eds1* null mutants to *P. parasitica* in accessions L*er* (*eds1-2*) and Ws-0 (*eds1-1*) (Figures 3A and 3B). A null *eds1* mutant in Col-0 was not available for phenotypic

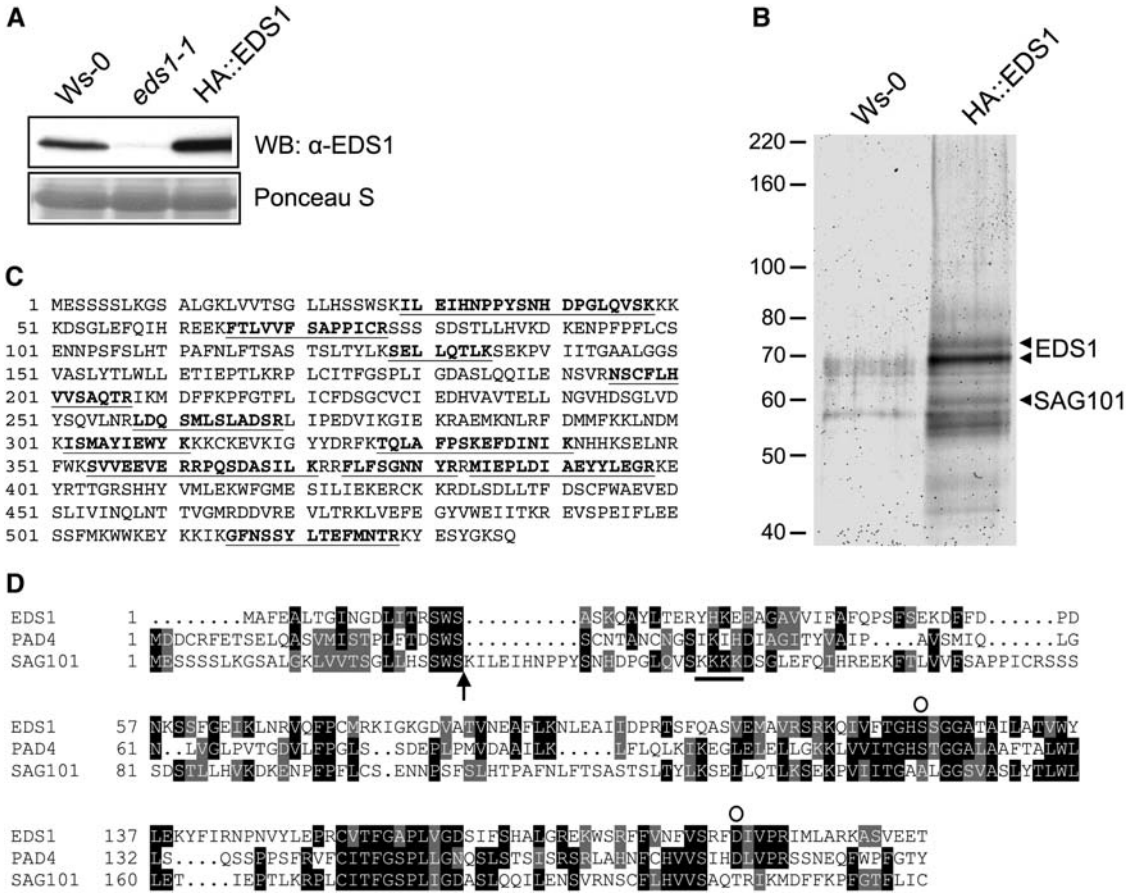

Figure 1. Identification of SAG101 as an EDS1-Interacting Protein in *Arabidopsis* Leaf Soluble Extracts.

(A) Protein gel blot analysis showing levels of HA-tagged EDS1 in a transgenic *eds1-1* line used for affinity purification of EDS1 complexes. Ponceau S staining of the membrane shows equal loading.

(B) EDS1-interacting proteins were purified from 5-week-old leaves of the HA-tagged EDS1 line or from Ws-0 as a control. Interacting proteins were eluted, separated by SDS-PAGE, and stained with colloidal Coomassie blue. Differential bands (arrowheads) were isolated and identified by mass spectrometry. Molecular mass markers (kilodaltons) are shown at left.

(C) SAG101 protein sequence from accession Col-0 showing peptides identified by Q-TOF tandem mass spectrometry analysis of the protein band isolated in **(B)**.

(D) Sequence alignment of the N-terminal lipase-like domains of EDS1, PAD4, and SAG101. A predicted signal peptide cleavage position in SAG101 is indicated with an arrow. A potential SAG101 nuclear localization sequence is underlined. Open circles show the positions of predicted Ser hydrolase catalytic residues in EDS1 and PAD4 and their apparent absence in SAG101.

comparison within the same genotype. Basal resistance to virulent *P. parasitica* isolate Noco2 was significantly more disabled in *pad4-1 sag101-2* plants than in *pad4-1* alone (Figure 3B). The genetic requirement for combined *PAD4* and *SAG101* in *Arabidopsis* resistance to avirulent strains of the bacterial pathogen *Pseudomonas syringae* pv *tomato* strain DC3000 was also tested. Resistance mediated by the TIR-type NB-LRR *R* gene, *RPS4*, to DC3000 expressing *avrRps4* was abolished in *pad4-1 sag101* lines, whereas resistance conferred by the CC-NB-LRR gene, *RPM1*, to DC3000 expressing *avrRpm1* remained intact (Figures 4A and 4B). Basal resistance to virulent DC3000 was suppressed equivalently in *pad4-1* and *pad4-1 sag101* lines (Figure 4C). These results show that the combined activities of PAD4 and SAG101 are essential for full resistance and programmed cell death triggered by TIR-type NB-LRR proteins and the expression of basal defenses against virulent *P. parasitica*. We conclude that SAG101 contributes significant activity to the EDS1-regulated resistance pathway. This pathway is either not needed or can be overridden in *RPM1* signaling.

EDS1, PAD4, and SAG101 Proteins Are Stabilized by Their Interacting Partners

We tested whether EDS1 is required for the accumulation of PAD4 and/or SAG101 because it associates with both proteins in vivo. In targeted yeast two-hybrid experiments, SAG101 interacted with EDS1 but did not interact with PAD4 (data not shown).

An *Arabidopsis* line carrying c-Myc–tagged PAD4 driven by its native promoter (referred to as Myc-PAD4; see Methods) (Feys et al., 2001) was crossed into the *eds1-1 pad4-5* background.

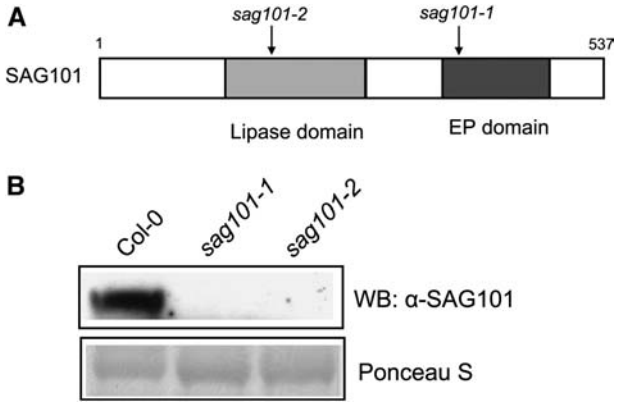

Figure 2. Characterization of *Arabidopsis sag101* Mutants.

(A) Scheme of the SAG101 protein showing the positions of two independent dSpm transposon insertions isolated in accession Col-0.
(B) Protein gel blot analysis of SAG101 in *sag101* knockout lines. Total leaf protein was isolated from unchallenged 4-week-old plants and analyzed with anti-SAG101 antibodies. Ponceau S staining of the membrane shows equal loading.

Myc-PAD4 protein was severely depleted in the absence of EDS1 (Figure 5A), a faint band being detected only after long exposure of the protein gel blots. Analysis of the same line for SAG101 protein accumulation also showed a severe depletion of SAG101 (Figure 5B). Thus, there is an absolute requirement for EDS1 in PAD4 and SAG101 accumulation. By contrast, mutations in PAD4 did not deplete SAG101 (Figure 5B). RT-PCR analysis of the same material revealed that the expression of *SAG101* and *PAD4* mRNAs was similar in *eds1* mutant and the wild type (data not shown), indicating that EDS1 acts posttranscriptionally and probably at the level of SAG101 and PAD4 protein accumulation. The Myc-PAD4 line was crossed to *sag101-2*, and a homozygous *pad4-5 sag101-2* line carrying Myc-PAD4 was selected. In this background, Myc-PAD4 attained ~50% levels seen in the parental Myc-PAD4 line (Figure 5C). Thus, the absence of SAG101 partially depletes the PAD4 pool, but not vice versa. EDS1 was depleted incrementally in *sag101*, *pad4*, and *pad4 sag101* leaf tissues, although residual EDS1 (~10% of the levels in wild-type tissues) was detected in the absence of both PAD4 and SAG101 (Figure 5D). These data show that EDS1, PAD4, and SAG101 have mutually stabilizing effects on their interacting partners. SAG101 and PAD4 contribute additively to EDS1 accumulation. However, because SAG101 and PAD4 have little effect on each other's accumulation but strictly require EDS1, we reasoned that EDS1–SAG101 and EDS1–PAD4 may form separate complexes.

SAG101 and PAD4 Have Defense Regulatory Functions beyond Stabilizing EDS1

From the pathogen assay (Figures 3 and 4) and protein gel blot (Figure 5) data, we thought that diminished resistance in *pad4-1* and *pad4 sag101* double mutants might reflect the stabilization of EDS1. In this scenario, EDS1 would be the key signal transducer, and reducing EDS1 below a certain threshold (Figure 5D) could account for increased disease susceptibility. To test this hypothesis, we compared the levels of extractable EDS1 in *pad4 sag101* and in a Col-0 line in which endogenous *EDS1* was stably silenced using a double-stranded RNA interference (dsRNAi) construct. Characterization of this line (denoted Col-*eds1*RNAi) by RT-PCR showed that mRNAs of two Col-0 *EDS1* genes (*EDS1A* [At3g48090] and *EDS1B* [At3g48080] lying in tandem on the lower arm of chromosome 3) with high sequence identity (82%) were almost undetectable compared with the wild type, whereas *PAD4* and *SAG101* expression was unaffected (data not shown). EDS1 protein in Col-*eds1*RNAi accumulated to significantly lower levels than in *pad4 sag101* (Figure 6A). However, Col-*eds1*RNAi leaves exhibited stronger *RPP2* resistance than *pad4-1 sag101* in response to *P. parasitica* isolate Cala2 (Figure 6B). We conclude that PAD4 and SAG101 have intrinsic signaling capabilities beyond stabilizing EDS1 in TIR-NB-LRR–type *R* gene–triggered resistance. The Col-*eds1*RNAi line displayed a similar degree of susceptibility as *pad4 sag101* to virulent *P. parasitica* isolate Noco2 (Figure 6B), suggesting that maintenance of a certain EDS1 threshold or induction of EDS1 is important for the full expression of basal resistance.

EDS1–PAD4 and EDS1–SAG101 Form Distinct Protein Complexes

We have gathered evidence for in planta protein complexes containing EDS1 plus PAD4 (Feys et al., 2001) and EDS1 plus SAG101 (presented here). EDS1 is also capable of homodimerization in yeast (Feys et al., 2001). To examine the nature of EDS1–SAG101 and EDS1–PAD4 associations in plant tissues, we first looked at the migration of EDS1-, PAD4-, and SAG101-containing protein complexes in leaf soluble extracts of pathogen-unchallenged plants separated by size exclusion chromatography. In the wild type, the bulk of EDS1 migrated at an apparent size of ~120 kD, consistent with the presence of EDS1 homodimers and/or heterodimers (Figure 7A, panels 1 and 8). A tail of EDS1 migrating more slowly may represent a small pool of monomeric EDS1. A potential monomeric EDS1 pool is seen more clearly in the *sag101* mutant (Figure 7A, panel 9). The migration profile of EDS1 in the Myc-tagged PAD4 transgenic line was identical to that in nontransgenic Ws-0 (Figure 7A, panel 3). Myc-PAD4 migrated as a higher molecular mass (~200 kD) pool (Figure 7A, panel 4). Immunoprecipitation of EDS1 complexes in individual column fractions followed by detection with anti-c-Myc confirmed the presence of an EDS1–PAD4 complex in all fractions containing Myc-PAD4 (Figure 7A, panel 5). We concluded that only a small fraction of the total EDS1 forms a stable complex with PAD4 in pathogen-unchallenged tissues. From these data, we could not distinguish whether the PAD4 complex contains dimeric EDS1, EDS1 and SAG101, or EDS1 in combination with an as yet unidentified component(s). In contrast to PAD4, SAG101 protein migrated with the principal 120-kD pool of EDS1 (Figure 7A, panel 6), suggesting that most SAG101 associates with EDS1 in a complex that does not include PAD4. Consistent with this notion, SAG101 total amounts (Figure 5B) and migration (Figure 7A, panel 7) were

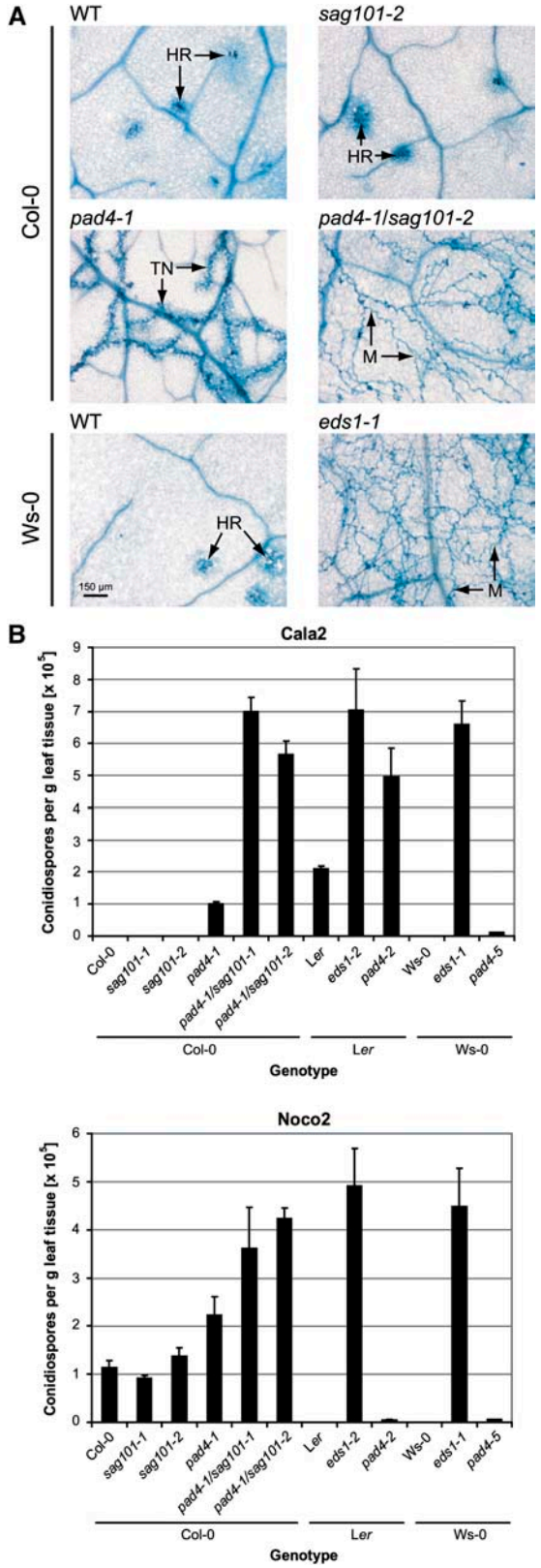

Figure 3. Loss of *RPP2* and Basal Resistance in *pad4 sag101* Mutants.

Two-week-old seedlings were spray-inoculated with *P. parasitica* conidiospores (4×10^4/mL), and pathogen development was recorded.

(A) Infection phenotypes of leaves inoculated with *P. parasitic*a isolate Cala2. Leaves were stained with lactophenol trypan blue 7 d after inoculation to visualize pathogen mycelium and necrotic plant cells. HR, hypersensitive response; M, mycelium; TN, trailing necrosis.

(B) Sporulation levels of *P. parasitica* isolates Cala2 and Noco2 on *Arabidopsis* wild-type and mutant lines. *pad4 sag101* double mutants permit pathogen sporulation to levels equivalent to those on *eds1-1* and *eds1-2*. Spores were harvested from leaves and counted 6 d after inoculation. Top, Cala2 is recognized by *RPP2* in Col-0 and by *RPP1A* in Ws-0 but is virulent on L*er*. Bottom, Noco2 is virulent on Col-0 but recognized by *RPP5* in L*er* and by *RPP1* in Ws-0. Backgrounds are L*er* for *eds1-2* and *pad4-2* and Ws-0 for *eds1-1* and *pad4-5*. Experiments were repeated twice with similar results. Bars represent means + SD.

not altered significantly in *pad4* extracts. Also, supporting the protein gel blot analysis (Figure 5), EDS1 levels on the size exclusion column were significantly reduced in *pad4-5* (Figure 7A, compare panels 1 and 2), in *sag101-2* (Figure 7A, compare panels 8 and 9), and most dramatically in the *pad4-1 sag101-2* double mutant (Figure 7A, compare panels 8 and 10). However, the EDS1 migration profile was not changed dramatically in these mutants. Residual EDS1 in the ~120-kD range in *sag101-2* may reflect the presence of EDS1 homodimers. Interestingly, although Myc-PAD4 associates with only a minor fraction of the total EDS1 pool in higher molecular mass fractions, both *pad4-5* and *pad4-1* mutations caused a significant reduction of EDS1 in the ~120-kD complexes (Figure 7A, compare panels 1 and 2 and panels 9 and 10). This finding suggests a degree of coregulation between individual EDS1 complexes.

We conclude that several molecularly distinct EDS1 complexes exist in *Arabidopsis* leaf extracts and that PAD4 is part of a small, discrete higher molecular mass EDS1 pool. To test whether SAG101 could form part of the EDS1–PAD4 complex, we measured the migration of Myc-PAD4 in a *sag101-2* background, anticipating that this would cause a shift in the Myc-PAD4 signal to the size of the major EDS1 fraction. As can be seen from Figure 7B, there was no shift in Myc-PAD4 mobility in *sag101-2* extracts, suggesting that SAG101 does not form an integral part of the EDS1–PAD4 complex. Residual Myc-PAD4 protein in the *eds1-1* background shows a migration profile that is not substantially different from that of the wild type (Figure 7B).

Localization of EDS1–PAD4 and EDS1–SAG101 Complexes inside the Cell

Intracellular localizations of EDS1, PAD4, and SAG101 were examined to distinguish different EDS1 complexes spatially within the cell. *Arabidopsis eds1-1 pad4-5* leaves were cobombarded with DNA constructs containing EDS1 driven by the cauliflower mosaic virus 35S promoter and fused to a terminal yellow fluorescent protein (YFP) tag (35S:EDS1-YFP) and either 35S:PAD4-CFP (for cyan fluorescent protein) or 35S:SAG101-CFP. Fluorescence in individual epidermal cells was measured on a confocal laser scanning microscope 24 h after transfection. As shown in Figure 8A, EDS1-YFP and PAD4-CFP colocalized to

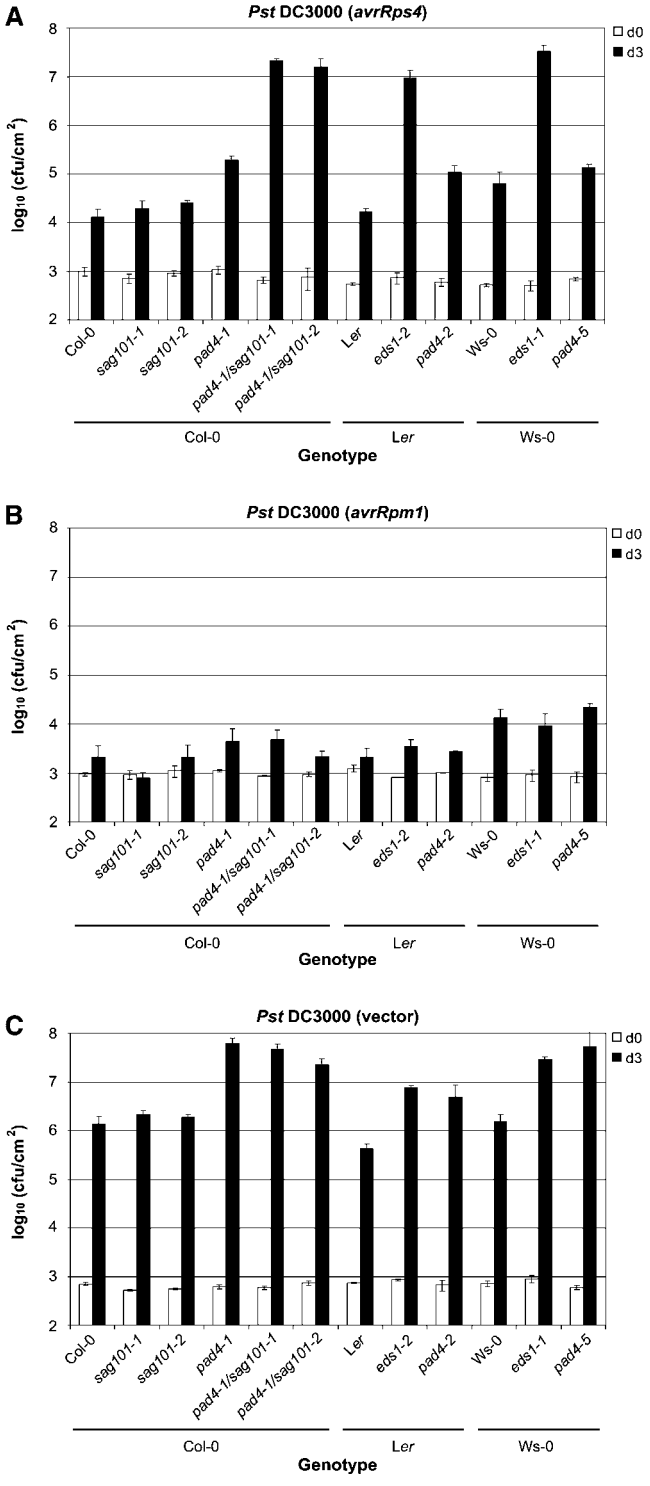

Figure 4. Growth of *P. syringae* pv *tomato* Strains in Leaves of Wild-Type and Mutant *Arabidopsis*.

Five-week-old plants of the indicated plant lines were vacuum-infiltrated with a bacterial suspension (5×10^5 colony-forming units [cfu]/mL) of avirulent *P. syringae* pv *tomato* (*Pst*) strain DC3000 expressing *avrRps4* **(A)**, *Pst* DC3000 expressing *avrRpm1* **(B)**, or virulent *Pst* DC3000 without an *avr* gene **(C)**. Bacterial titers were measured at d 0 (d0) and d 3 (d3).

Bacterial growth is expressed as mean values of viable bacteria per cm^2 of leaf tissue ± SD resulting from two replicate samplings for d0 and three replicate samplings for d3.

both the cytosol and the nucleus, whereas SAG101-CFP was found only in the nucleus. The same distributions were observed if these genes were bombarded individually, although a stronger EDS1-YFP signal was obtained in the nucleus when cobombarded with SAG101-CFP than when bombarded alone or in combination with PAD4-CFP (Figure 8A). Confocal sectioning through the images revealed that all three proteins were present inside the nucleus rather than on its periphery (Figure 8A). A proportion of EDS1-YFP was still observed inside the nuclei after bombardment into *sag101* or *pad4 sag101* cells (see Supplemental Figure 1A online), indicating that EDS1 is not dependent on SAG101 or PAD4 to enter the nucleus. To exclude the possibility that the transiently overexpressed proteins were mislocalized, nuclei were purified from Col-0 or the Myc-PAD4 transgenic line and the presence of EDS1, SAG101, and Myc-PAD4 was determined on protein gel blots of nuclear extracts. EDS1 and Myc-PAD4 were found in nuclear as well as in supernatant fractions from which nuclei had been removed, whereas SAG101 was detectable only in nuclear fractions (Figure 8B). We conclude that the intracellular localizations deduced from transient expression upon particle bombardment of fluorescent protein–tagged EDS1, PAD4, and SAG101 likely reflect their physiological locations in the cell. We reasoned further that EDS1–SAG101 complexes must be nuclear, whereas EDS1–PAD4 and potentially EDS1–EDS1 interactions could occur in both the cytosol and the nucleus.

We used transient bombardment assays of the fluorescent protein–tagged forms to measure direct protein–protein interactions in different cellular compartments of *Arabidopsis* epidermal cells by FRET and acceptor photobleaching (APB) (Karpova et al., 2003). A specific FRET signal was obtained in nuclei between EDS1-CFP and SAG101-YFP (Figure 8C). Thus, EDS1 and SAG101 associate directly inside the nucleus. Specific FRET signals were also measured between EDS1-CFP and EDS1-YFP at sites in the cytosol, indicating that EDS1 dimerizes in this compartment (Figure 8D). FRET signals between EDS1-CFP and EDS1-YFP were not above background when measured in the nucleus (Figure 8D), suggesting a difference in the nature of homomeric EDS1 interactions between these two compartments. We were unable to measure consistent FRET above background controls between EDS1-CFP and PAD4-YFP in the cytosol or the nucleus (see Supplemental Figure 1B online).

DISCUSSION

Arabidopsis EDS1 constitutes a central regulatory node in innate immunity, controlling the accumulation of salicylic acid and other defense molecules to drive basal resistance and connecting TIR-NB-LRR–mediated pathogen recognition to downstream defense activation. We identify here a new component of the EDS1 pathway, SAG101, that interacts with EDS1 in the nucleus and cannot accumulate without EDS1. Significantly, the SAG101

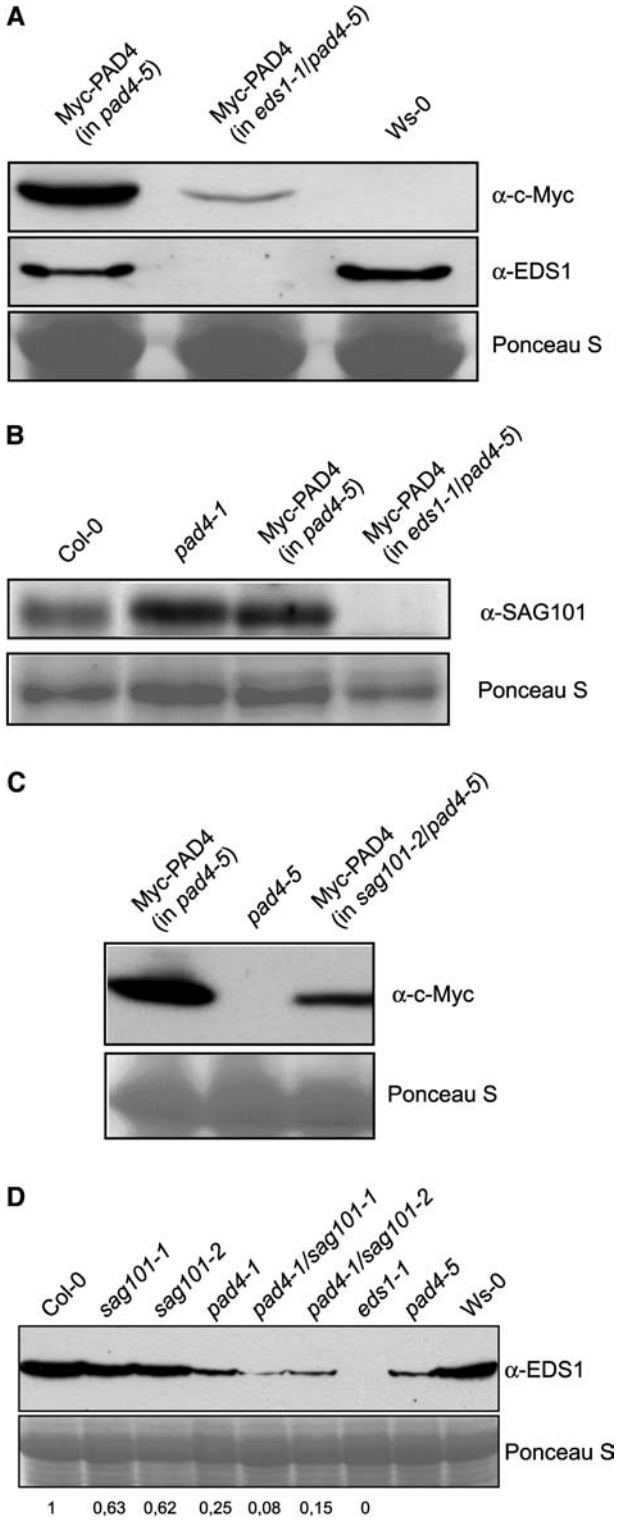

Figure 5. EDS1, PAD4, and SAG101 Proteins Are Stabilized by Their Interacting Partners.

Protein gel blot analysis of total protein extracts derived from 4-week-old unchallenged leaves of different *Arabidopsis* lines. Equal loading is shown by Ponceau S staining of the membranes.

(A) Accumulation of Myc-PAD4 requires EDS1.

(B) SAG101 protein requires EDS1 but not PAD4 for accumulation. Equal amounts of total soluble protein of the indicated lines were separated by gel filtration, and SAG101-containing fractions were pooled and analyzed by protein gel blotting.

(C) Maximal Myc-PAD4 accumulation depends on SAG101.

(D) EDS1 protein is depleted incrementally in *pad4*, *sag101*, and *pad4 sag101* backgrounds. Numbers below the blot indicate band intensities relative to the EDS1 signal obtained for wild-type Col-0, as measured by ImageQuant 5.2 software.

sequence determined by Q-TOF tandem mass spectrometry in our study differs at the N terminus from a previously published SAG101 sequence (He and Gan, 2002). Although we cannot exclude the possibility that this is attributable to accession-specific polymorphisms, the open reading frame shown here was confirmed by RT-PCR and encodes a protein that interacts in vivo with EDS1. SAG101 possesses a predicted signal peptide cleavage site that is not found in either EDS1 or PAD4 (Figure 1D), although it is unclear whether a processed form of SAG101 accumulates in plant cells. Because *SAG101* had been implicated previously in the regulation of leaf senescence in *Arabidopsis* accession Col-*glabrous1* (He and Gan, 2002), we tested both *sag101* dSpm insertion mutants for alterations in visible onset and progression of leaf senescence. We detected no significant differences from the wild type and also observed no senescence-associated phenotypes in Ws-0 *eds1-1* (no detectable SAG101 protein; Figure 5B) or L*er eds1-2* (B.J. Feys, unpublished data).

SAG101 contributes to the EDS1 defense signaling pathway. Genetically, *SAG101* and *PAD4* are partially redundant. Loss of *SAG101* can be compensated for by the presence of *PAD4* in both TIR-NB-LRR–type *R* gene–triggered and basal resistance (Figures 3 and 4). *SAG101* is not as efficient in compensating for the absence of *PAD4*, implying a unique capability of PAD4, potentially as a consequence of differential cellular localization. We reasoned that this PAD4 activity is in combination with EDS1, because PAD4 depends on EDS1 for accumulation and all of the detectable PAD4 protein pool is associated with EDS1, at least in unchallenged cells (Figures 5 and 7). The sum of PAD4 and SAG101 activities is at least equivalent to that of EDS1, because *pad4 sag101* mutants, like *eds1*, are completely disabled in *RPP*-mediated resistance to *P. parasitica* (Figure 3) and *RPS4* resistance to *P. syringae* (Figure 4A). Indeed, the *pad4 sag101* combination appears to create a supersusceptible background to virulent *P. parasitica* (Figure 3B), because the double mutant exhibited a greater loss of basal resistance than *pad4-1*, a null mutation in accession Col-0 (Jirage et al., 1999). In other *Arabidopsis* accessions (Ws-0 and L*er*), *pad4* disables basal resistance and blocks reactive oxygen intermediate–derived signal potentiation as fully as *eds1*, suggesting equal contributions of EDS1 and PAD4 to these processes (Rustérucci et al.,1999; Mateo et al., 2004).

The genetic interplay of *EDS1*, *PAD4*, and *SAG101* combined with a stringent requirement for EDS1 to stabilize both PAD4 and SAG101 implies that EDS1 may act as an adaptor or scaffold for these two components to ensure appropriate signal relay

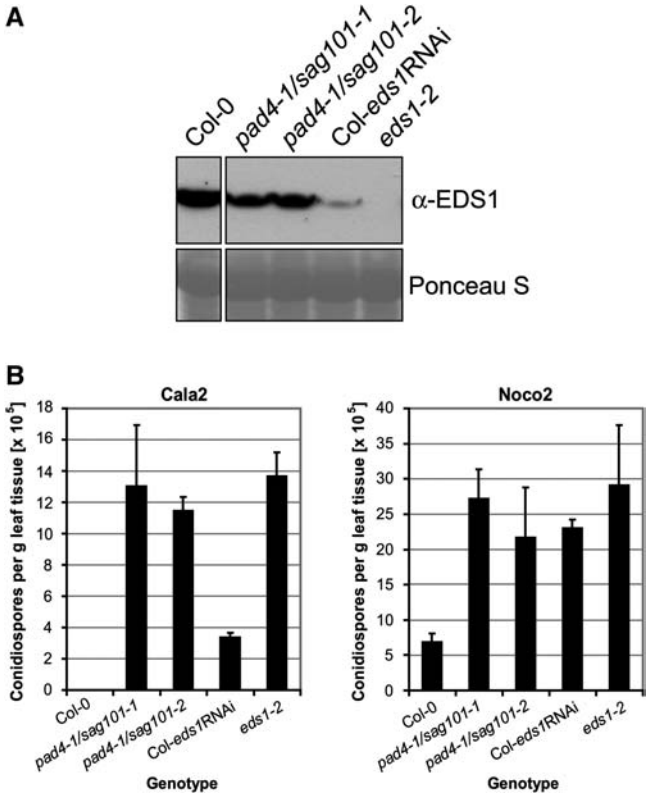

Figure 6. Infection Phenotypes of *Arabidopsis* Mutants Depleted in EDS1.

(A) EDS1 abundance in total protein extracts from 4-week-old unchallenged leaves of the indicated *Arabidopsis* lines. All mutants are in Col-0, except *eds1-2* (L*er*). Equal loading is shown by Ponceau S staining of the membrane.

(B) Sporulation levels of *P. parasitica* isolates Cala2, recognized by *RPP2* (left), and virulent Noco2 (right) on *Arabidopsis* lines tested in **(A)**. Two-week-old seedlings were spray-inoculated with *P. parasitica* conidiospores, and spores were counted as described for Figure 3. Experiments were repeated twice with similar results. Bars represent means + SD.

(Park et al., 2003). PAD4 and SAG101, in an incremental manner, also stabilize EDS1 (Figure 5), consistent with the presence of distinct EDS1–PAD4 and EDS1–SAG101 pools in pathogen-unchallenged cells. We considered two possible roles for PAD4 and SAG101. In one model, they structurally stabilize EDS1, which is the principal signaling moiety. In the other model, they contribute intrinsic signaling activity to the EDS1 complexes in which they reside. We favor the latter model, because depleting EDS1 protein in the Col-*eds1*RNAi line to almost undetectable levels did not compromise resistance as fully as removing both SAG101 and PAD4 in *pad4 sag101*, even though the residual EDS1 level in *pad4 sag101* was higher than that in Col-*eds1*RNAi (Figure 6). Therefore, it is likely that all three components are important for signal relay. Importantly, SAG101 and PAD4 are necessary for the transduction of signals triggered by activated TIR-NB-LRR proteins leading to programmed cell death (Figures 3 and 6). Low amounts of EDS1 (Figure 6) may serve to transduce a signal from TIR-NB-LRR proteins to PAD4 and SAG101, which, coupled to EDS1, amplify the defense response. Such amplification involving the upregulation of *EDS1* and partners (Zhou et al., 1998; Jirage et al., 1999; Feys et al., 2001; Xiao et al., 2003; Chandra-Shekara et al., 2004) may be critical for the full expression of basal resistance. The biochemical modes of action of EDS1 and its partners in these processes remain unclear, although stable *Arabidopsis* transgenic lines expressing EDS1 and PAD4 variants with exchanges of the predicted lipase catalytic residues were not compromised in resistance (B.J. Feys and J.E. Parker, unpublished data). Also, we were unable to detect lipase activities in EDS1, PAD4, or SAG101 proteins expressed in *E. coli* (S. Rietz and J.E. Parker, unpublished data). The apparent dispensability of these catalytic amino acids in EDS1 and PAD4 and their absence in wild-type SAG101 (Figure 1D) but retention of the lipase domains in all plant homologs examined to date suggest that they may fulfill a structural rather than an enzymatic role, as discovered for some other signaling proteins (Llompart et al., 2003; Wang et al., 2003; Lu et al., 2004).

To reveal the signaling functions of EDS1 and its partners, it was important to determine their locations in the cell and the nature of the EDS1–PAD4 and EDS1–SAG101 associations. We could resolve molecularly and spatially distinct complexes. The entire cellular pool of PAD4 (determined by size exclusion chromatography) associates with a small proportion of total EDS1 in an ~200-kD complex that can be distinguished from the majority of EDS1 and SAG101 (Figure 7). The EDS1–PAD4 complex does not appear to contain SAG101 because there is no shift of Myc-PAD4 toward a lower molecular mass pool in *sag101* mutants (Figure 7B). This conclusion is supported by the finding that EDS1, but not SAG101 protein, could be coimmunoprecipitated with Myc-PAD4 from soluble cell extracts (M. Wiermer, unpublished data). The EDS1–PAD4 complex may be partially composed of EDS1 homodimers identified by FRET analyses of transiently expressed EDS1-CFP and EDS1-YFP in epidermal cells (Figure 8; see below) or other, as yet unknown, components. Besides PAD4 and SAG101, no other proteins that are highly sequence-related to EDS1 were found in the *Arabidopsis* genome. An alternative explanation is that the physicochemical nature of an EDS1–PAD4 complex alters its mobility on the size exclusion column.

EDS1 and PAD4 localized to the cytosol and nucleus, whereas SAG101 was detected only in the nuclear compartment after transfection of fluorescent protein–tagged proteins into *Arabidopsis* epidermal cells. Similar partitioning of these proteins in cellular fractionation experiments of wild–type or Myc-PAD4 tissues suggests that the transiently expressed proteins are localized correctly. Moreover, a C-terminal fluorescent protein tag does not appear to interfere with EDS1 and PAD4 function in stable primary transformants of *eds1-1* and *pad4-5* expressing the fusion proteins under their respective native promoter (M. Wiermer and J.E. Parker, unpublished data). Analysis of the stable transgenic lines revealed that EDS1-YFP has a nuclear-cytoplasmic localization, as seen in the bombardment assays, whereas PAD4-CFP fluorescence is not detectable (M. Wiermer and J.E. Parker, unpublished data). Restriction of SAG101 to the nucleus may account for its inability to fully complement the loss of PAD4. If this is the case, it follows that a cytosolic EDS1–PAD4 complex, and/or passaging of EDS1 and PAD4 between these two compartments, is important for signal relay. Mobility

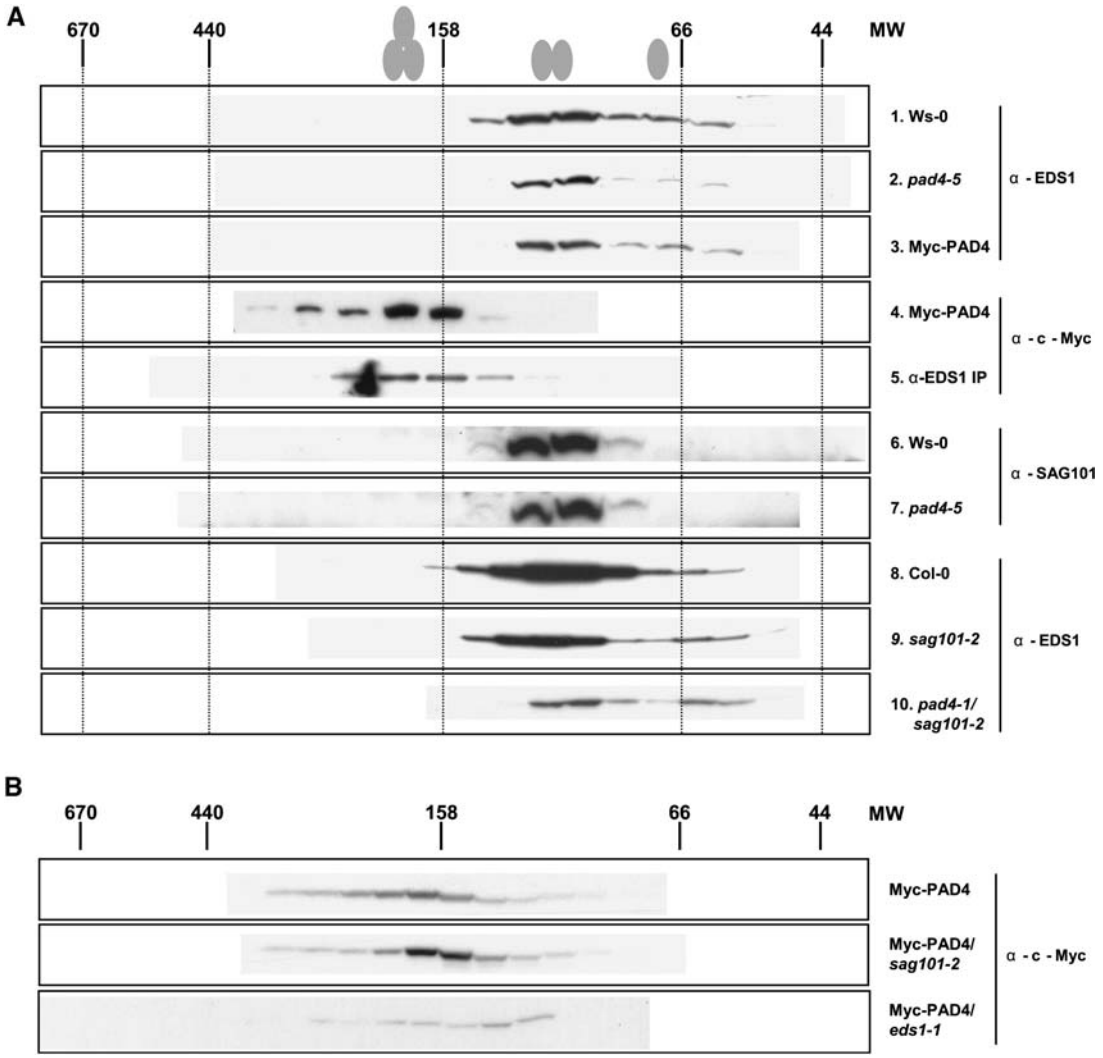

Figure 7. Distinct EDS1 Complexes Are Present in Soluble Leaf Extracts.

Size exclusion chromatography was used to separate total soluble protein extracted from 5-week-old unchallenged leaves of the indicated lines. Individual fractions from a Superdex 200 16/60 column were analyzed for the presence of EDS1-, Myc-PAD4–, and/or SAG101-containing complexes. Schemes of possible monomeric, dimeric, and trimeric protein associations are shown at top. Equal amounts of total protein per line were separated for each gel filtration experiment.

(A) Profiles of EDS1, PAD4, and SAG101 protein complexes in wild-type and mutant lines.

(B) Effect of *sag101-2* and *eds1-1* mutations on apparent Myc-PAD4 complex size. Removal of SAG101 or EDS1 protein does not significantly alter apparent Myc-PAD4 complex size. The top gel was exposed for 1 min, the middle gel was exposed for 5 min, and the bottom gel was exposed for 10 min to compensate for overall reduced Myc-PAD4 protein levels in *sag101* and *eds1* mutants.

between the cytosol and the nucleus is an essential feature of another plant defense regulator, NPR1, an ankyrin-repeat protein that controls basal and systemic resistance downstream of salicylic acid (Mou et al., 2003). The recent identification of a nucleoporin-like protein, MOS3, as a component of EDS1- and PAD4-dependent TIR-NB-LRR–triggered and basal resistance also indicates the importance of nuclear-cytoplasmic trafficking in plant defense signaling (Zhang and Li, 2005).

We were unable to detect a physical EDS1–PAD4 association by FRET in bombarded *Arabidopsis* epidermal cells, even though these proteins interact in a yeast two-hybrid assay and coimmunoprecipitate in leaf soluble extracts (Feys et al., 2001; M. Wiermer, unpublished data). Their binding affinities may be too weak to be detected by FRET (see Supplemental Figure 1B online). This feature, coupled with the low abundance of the EDS1–PAD4 complex (Figure 7), may explain our failure to detect PAD4 peptides by Q-TOF mass spectrometry analysis of EDS1 interactors. Alternatively, the molecular orientations of the fluorescent protein tags might preclude the transfer of fluorescence energy. Another possibility is that a third protein (which would have to be conserved in yeast) bridges between EDS1 and PAD4 (see above). Whatever the precise nature of the EDS1–PAD4

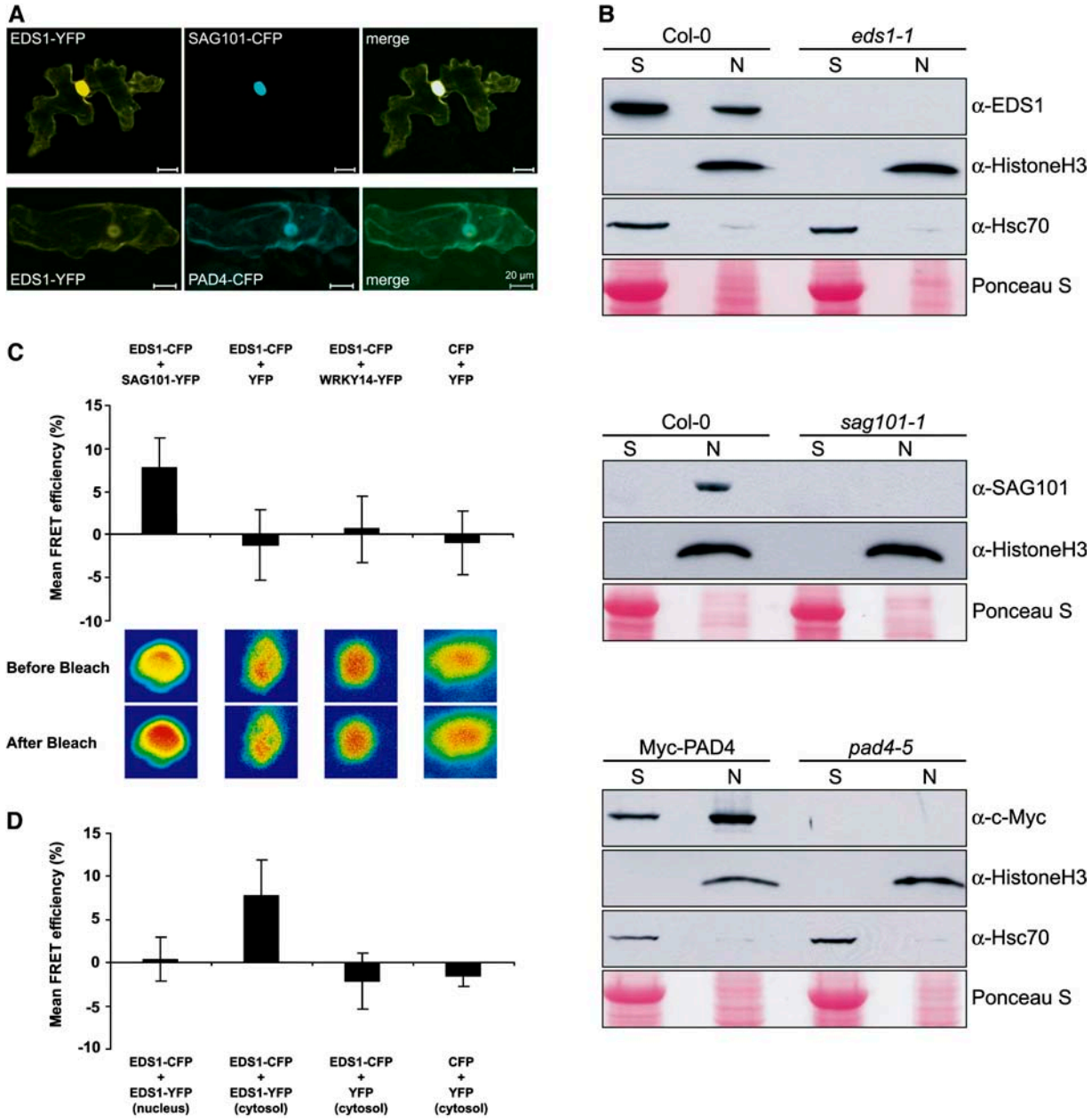

Figure 8. Subcellular Localizations and FRET Interaction Studies of EDS1, SAG101, and PAD4.

(A) *Arabidopsis* epidermal cells were cotransfected with fluorescently tagged EDS1 and SAG101 (top row) or EDS1 and PAD4 (bottom row) and analyzed by confocal laser scanning microscopy. Images shown are three-dimensional reconstructions from individual image stacks.

(B) Protein gel blot analysis of EDS1, SAG101, and Myc-PAD4 in subcellular fractions of unchallenged leaf tissues. Histone H3 was used as a nuclear marker, and cytosolic Hsc70s served as a cytosolic marker. N, nuclear protein extracts; S, total protein extracts depleted of nuclei.

(C) FRET-APB analysis of the interaction in nuclei between EDS1-CFP and SAG101-YFP. Mean FRET efficiencies ± SD from individual sample sites (>30 for EDS1–SAG101 and 10 to 20 for controls) are shown. Representative images of pseudocolored nuclei show donor fluorescence before and after bleaching for each cotransfection. An increase of donor fluorescence (red) is seen only if protein–protein interaction occurs.

(D) FRET-APB analysis of the interaction between EDS1-CFP and EDS1-YFP. Mean FRETefficiencies ± SD from individual sample sites (20 for EDS1–EDS1 and 15 for controls) are shown.

complex, it represents a small but potent EDS1 signaling pool in the cell. It also appears to communicate intimately with the more abundant EDS1 pool, because removing PAD4 in *pad4-1* and *pad4-5* plants reduces substantially the total EDS1 content but does not deplete SAG101 (Figures 5 and 7). Curiously, PAD4 is depleted by ~50% in *sag101*, whereas SAG101 levels are unchanged in *pad4* (Figure 5). Thus, although not part of the EDS1–PAD4 complex, SAG101 may change the molecular character of EDS1 in some way that promotes PAD4 binding.

EDS1 dimerization and EDS1–SAG101 associations were resolved spatially by measuring specific FRET signals between transiently expressed fluorescent protein–tagged proteins in individual *Arabidopsis* epidermal cell compartments. Strong EDS1–SAG101 binding occurred inside the nucleus (Figure 8C). Significantly, EDS1 homodimerization was recorded in the cytosol but not in the nucleus (Figure 8D). The absence of detectable EDS1 homodimers in the nucleus implies a difference in EDS1 interaction dynamics between these two cellular compartments. This may be attributable to the presence of SAG101, which might compete with EDS1 dimers for binding, or may be a consequence of differential recruitment to the nucleus as a result of differences in the accessibility of nuclear localization signals. EDS1-YFP fluorescence was consistently stronger in the nucleus and weaker in the cytosol after cobombardment with SAG101-CFP than after bombardment of EDS1-YFP with PAD4-CFP or alone (Figure 8), suggesting that EDS1 may be preferentially held inside the nucleus by SAG101 once it has entered this compartment, although the ability of EDS1 to enter the nucleus does not depend on SAG101 or PAD4 (see Supplemental Figure 1A online). These new findings suggest an intricate cellular dynamic between EDS1 and its signaling partners and lead us to speculate that changes in the nature and/or distribution of these complexes in response to a pathogen stimulus may be critical in defense signal transmission.

METHODS

Plant Materials, Pathogen Isolates, and Pathology Assays

Arabidopsis thaliana wild-type accessions and mutant lines have been described (Jirage et al., 1999; Feys et al., 2001). For selection of the Col-0 dSpm lines *sag101-1* and *sag101-2*, the SLAT collection (Tissier et al., 1999) was screened for insertions in the *SAG101* gene by PCR using the *SAG101*-specific primers BF52 (5′-CACGCGTCCGAAGATCTTGGAGATACATA-3′) and BF53 (5′-ACTTCCGGGTGTTCATAAACTCGGTCAAG-3′) in combination with the *dSpm*-specific primers dSpm1 (5′-CTTATTTCAGTAAGAGTGTGGGGTTTTGG-3′) and dSpm11 (5′-GGTGCAGCAAAACCCACACTTTTACTTC-3′). The *pad4 sag101* double mutant was generated by crossing *sag101-1* and *sag101-2* lines to *pad4-1* followed by PCR identification of homozygous double mutants in the F2 generation using *sag101*-specific primers and a *pad4-1* codominant polymorphic DNA (CAPS) marker (primers 5′-TAGCTACCAAGCTGGTGTTGCGTTAG-3′ and 5′-CATTTTGCACTTGAACTCTTTCAGATTC-3′; diagnostic restriction enzyme *Bsm*FI). For generation of the *Myc-PAD4* transgenic line used in these experiments, a construct containing the full *PAD4* open reading frame fused in frame at the N terminus to five consecutive c-Myc epitope tags, driven by the endogenous *PAD4* promoter and flanked at the 3′ end by the nopaline synthase terminator (previously described in Feys et al., 2001), was generated and cloned into the BASTA resistance binary vector pGreenII 0229 (http://www.pgreen.ac.uk/pGreenII/pGreenII.htm) followed by the transformation of *pad4-5* plants by the floral dip method (Clough and Bent, 1998). Several independent *Myc-PAD4* transgenic lines were generated and shown to fully complement the *pad4-5* mutant. A representative line (internally referred to as LM41/2) was used for further analyses and crosses. To select *Myc-PAD4* in *pad4-5 eds1-1*, *Myc-PAD4* (in *pad4-5*) was crossed to *eds1-1 pad4-5*, and F1 plants were backcrossed to *eds1-1 pad4-5*. BC1 plants homozygous for *eds1-1 pad4-5* and containing the *Myc-PAD4* transgene were selfed, and a line homozygous for the transgene was selected. *Myc-PAD4* (in *pad4-5*) was also crossed to *sag101-2*, and a *pad4-5 sag101-2* line that was homozygous for the *Myc-PAD4* transgene was identified in the F2 generation by PCR. The Col-*eds1*RNAi line was made as follows. A silencing construct was generated using Gateway cloning technology (Invitrogen). Full-length *EDS1A* (At3g48090) cDNA (1872 bp) was amplified with specific primers and inserted via directional TOPO cloning into pENTR vector and recombined into the destination vector pJawohl8, a binary vector containing two inverted Gateway cassettes separated by the first intron of WRKY transcription factor 33 (At2g38470) designed to produce double-stranded RNA in plants. The *EDS1* dsRNAi construct was transferred to *Agrobacterium tumefaciens* strain GV3101 (pMP90RK) and used to transform *Arabidopsis* (ecotype Col-0) by the floral dip method (Clough and Bent, 1998). Transformants were selected on soil after spraying with phosphinotricin herbicide (Tissier et al., 1999). *Peronospora parasitica* isolates Cala2, Noco2, and Emwa1 were maintained and inoculated onto 2-week-old plants as described (Aarts et al., 1998). To determine pathogen conidiospore numbers, replicate samples of 30 seedlings were harvested 6 d after inoculation, vortexed in water, and counted in a hemocytometer on a light microscope. The extent of plant cell necrosis and the development of *P. parasitica* hyphae in leaf tissues were monitored 7 d after infection by staining with lactophenol trypan blue (Aarts et al., 1998). *Pseudomonas syringae* virulent and avirulent DC3000 strains used were as described (Aarts et al., 1998). Suspensions of 5×10^5 colony-forming units per milliliter in 5 mM $MgCl_2$ solution containing 0.002% (v/v) Silwet L-77 were vacuum-infiltrated into leaves of 5-week-old *Arabidopsis* plants, and leaves were sampled at 1 h and 3 d (Aarts et al., 1998).

Transgenic *Arabidopsis* Expressing HA- and TAP-Tagged EDS1

A 5.7-kb genomic DNA fragment containing L*er EDS1* (Falk et al., 1999) was used to generate affinity-tagged constructs. A single HA tag was generated by annealing of two complementary oligonucleotides (5′-AGATCCATGTACCCTTATGATGTGCCAGATTATGCCGGAGGTGG-3′ and 5′-CATGCCACCTCCGGCATAATCTGGCACATCATAAGGGTACATGGATCT-3′) and ligated to the unique *Bsa*BI site 14 bp upstream of the *EDS1* start codon and a PCR-generated L*er EDS1* genomic fragment containing an engineered *Nco*I site at the start codon and extending to the *Bst*XI site in the EDS1 open reading frame. This three-way ligation yielded genomic EDS1 with a single N-terminal HA tag driven by the endogenous promoter and flanked by the endogenous EDS1 3′ terminator. A *Xba*I/*Xcm*I fragment containing HA-tagged genomic EDS1 driven by 1.4 kb of endogenous promoter and containing EDS1 3′ sequence extending to the start of the next gene was cloned into the binary BASTA-selectable vector SLJ755I5 (Feys et al., 2001). Transformants of *eds1-1* were generated by the floral dip method (Clough and Bent, 1998). The same procedure was used to generate N-terminal TAP-tagged EDS1. The TAP tag was amplified from vector pBS1761 (a kind gift of Bertrand Seraphin; Rigaut et al., 1999) as a *Bsa*BI/*Nco*I fragment.

Affinity Purification and Mass Spectrometry

Leaf material of 5-week-old *Arabidopsis* plants was ground in liquid nitrogen and extracted in 50 mM Tris, pH 8, 150 mM NaCl, and 1 mM EDTA–containing protease inhibitor cocktail (P9599; Sigma-Aldrich).

Extracts were filtered and centrifuged at 100,000*g* to obtain total soluble fraction. Soluble protein (~500 mg) was rotated with high-affinity anti-HA agarose beads (Roche) or IgG beads (Amersham) and washed several times in extraction buffer. Bound proteins were eluted by boiling beads in 2× SDS sample buffer and fractionated on SDS-PAGE gels. Mass spectrometry was performed at the Joint IFR-JIC Proteomics Facility using standard procedures described at http://www.jic.bbsrc.ac.uk/services/proteomics/procedure.htm.

Size Exclusion Chromatography

Total protein extracts for gel filtration analyses were prepared as described above for affinity purifications. Total soluble protein (5 mg) was loaded onto a HiLoad Superdex 200 16/60 prep-grade column (Amersham) connected to an AKTA–fast protein liquid chromatography system (Amersham), and 2-mL fractions were collected. Individual fractions were concentrated to 50 μL in Amicon Ultra-4 centrifugal filter units (Millipore) and analyzed by protein gel blotting.

Protein Expression Analysis

Total protein extracts were prepared from leaves by homogenization in liquid nitrogen. Fifty-milligram samples were resuspended in 2× SDS-PAGE sample buffer and boiled for 5 min, and cell debris was removed by centrifugation before loading onto 10% SDS-PAGE gels. Proteins were electroblotted to nitrocellulose membranes for protein gel blot analysis. Equal loading was monitored by staining membranes with Ponceau S (Sigma-Aldrich). Polyclonal rabbit anti-EDS1 serum has been described (Feys et al., 2001). Rabbit anti-SAG101 polyclonal antibodies were generated against a mixture of two SAG101-specific peptides (393-YYLEGRKEYRTTGRS-407 and 525-MNTRKYESYGKSQ-537; BioGenes). After blocking in 10 mM Tris-HCl, 150 mM NaCl, and 0.05% Tween 20, pH 7.5, containing 5% blotting grade milk powder (Roth), membranes were incubated with primary antibodies: anti-EDS1, anti-c-Myc 9E10 (Santa Cruz Biotechnology), anti-SAG101, anti-histone H3 (Abcam), or anti-Hsc70 plant cytosolic (Stressgen Biotechnologies). Antibody-bound proteins were detected using a horseradish peroxidase–conjugated goat anti-rabbit or goat anti-mouse secondary antibody (Santa Cruz Biotechnology) using a chemiluminescence detection kit (Pierce). Nuclear fractionations were performed according to Kinkema et al. (2000). Protein gel blots of nuclear and supernatant fractions were probed as described above using anti-histone H3 and anti-Hsc70 antibodies, respectively, as nuclear and cytosolic markers.

Transient Expression of Fluorescent Protein–Tagged EDS1, PAD4, and SAG101 in *Arabidopsis* Epidermal Cells

To generate fluorescent protein destination vectors for Gateway cloning technology (Invitrogen), CFP and YFP were amplified by PCR from vector pMon999 (Shah et al., 2001). PCR products for CFP and YFP were ligated into the binary vector pXCS-HisHA containing the cauliflower mosaic virus constitutive 35S promoter (Witte et al., 2004), resulting in pXCS-CFP and pXCS-YFP. A Gateway recombination cassette was ligated into pXCS-CFP and pXCS-YFP, and the resulting clones, pXCSG-CFP and pXCSG-YFP, were selected. To fuse CFP or YFP to the C termini of EDS1, PAD4, SAG101, or a control protein, WRKY14, their respective sequences were cloned into pENTR/D-TOPO (Invitrogen) and recombined into pXCSG-CFP and pXCSG-YFP. Transient transfection of *Arabidopsis* epidermal cells by particle bombardment was performed as described (Shirasu et al., 1999). Briefly, detached 4-week-old leaves of plants grown on soil (10-h light period) were placed on 1% agar containing 85 μM benzimidazole and transfected using the particle delivery system Biolistic PDS-1000/He (Bio-Rad) with 900-p.s.i. rapture discs. For the simultaneous delivery of two constructs, equimolar plasmid mixtures were coated onto 1-μm gold particles. FRET analyses and fluorescence microscopy were performed 24 h after transfection.

Fluorescence Microscopy and FRET-APB

Confocal laser scanning microscopy on a LSM 510 META microscopy system (Zeiss) was performed to analyze intracellular fluorescence as described by Bhat et al. (2004). Colocalization studies and FRET-APB were performed as described previously (Karpova et al., 2003; Bhat et al., 2005). FRET efficiencies were calculated according to Karpova et al. (2003).

Accession Numbers

Sequence data from this article can be found in the GenBank/EMBL data libraries under accession numbers DQ103714 (full-length Col-0 SAG101 cDNA), AF128407 (L*er* genomic EDS1), AT3g48090 (Col-0 EDS1A), At3g48080 (Col-0 EDS1B), At2g38470 (pJaWohl8 binary vector), and AY436765 (pAMPAT-MCS).

ACKNOWLEDGMENTS

We thank Steffen Rietz for providing purified EDS1 antisera, B. Ülker for *WRKY14* cDNA, and Jonathan Jones (Sainsbury Laboratory) for use of the SLAT collection. We acknowledge the expert technical help of Mike Naldrett and colleagues at the Joint Institute for Food Research–John Innes Centre Proteomics Facility (funded in part by Biotechnology and Biological Sciences Research Council Joint Research Equipment Initiative Grants JRE10832, JE412701, and JE412631 and by grants from Syngenta and Unilever). We are grateful to R. Panstruga and P. Schulze-Lefert for helpful discussions. We acknowledge the Max Planck Society, the Alexander von Humboldt Foundation, and a Bundesministerium für Bildung und Forschung ''GABI-Nonhost'' grant for support. J.E.P. and B.J.F. also thank the Gatsby Foundation and the Biotechnology and Biological Sciences Research Council (Grant P13714) for funding.

Received May 3, 2005; revised June 14, 2005; accepted June 15, 2005; published July 22, 2005.

REFERENCES

Aarts, N., Metz, M., Holub, E., Staskawicz, B.J., Daniels, M.J., and Parker, J.E. (1998). Different requirements for *EDS1* and *NDR1* by disease resistance genes define at least two *R* gene-mediated signaling pathways in *Arabidopsis*. Proc. Natl. Acad. Sci. USA **95,** 10306–10311.

Bhat, R.A., Borst, J.W., Riehl, M., and Thompson, R.D. (2004). Interaction of maize Opaque-2 and the transcriptional co-activators GCN5 and ADA2, in the modulation of transcriptional activity. Plant Mol. Biol. **55,** 239–252.

Bhat, R.A., Miklis, M., Schmelzer, E., Schulze-Lefert, P., and Panstruga, R. (2005). Recruitment and interaction dynamics of plant penetration resistance components in a plasma membrane microdomain. Proc. Natl. Acad. Sci. USA **102,** 3135–3140.

Brodersen, P., Petersen, M., Pike, H.M., Olszak, B., Skov, S., Odum, N., Jorgensen, L.B., Brown, R.E., and Mundy, J. (2002). Knockout of *Arabidopsis ACCELERATED-CELL-DEATH11* encoding a sphingosine transfer protein causes activation of programmed cell death and defense. Genes Dev. **16,** 490–502.

Chandra-Shekara, A.C., Navarre, D., Kachroo, A., Kang, H.G., Klessig, D., and Kachroo, P. (2004). Signaling requirements and

role of salicylic acid in *HRT*- and *rrt*-mediated resistance to turnip crinkle virus in Arabidopsis. Plant J. **40,** 647–659.

Clough, S.J., and Bent, A.F. (1998). Floral dip: A simplified method for Agrobacterium-mediated transformation of *Arabidopsis thaliana*. Plant J. **16,** 735–743.

Falk, A., Feys, B.J., Frost, L.N., Jones, J.D.G., Daniels, M.J., and Parker, J.E. (1999). *EDS1*, an essential component of *R* gene-mediated disease resistance in *Arabidopsis* has homology to eukaryotic lipases. Proc. Natl. Acad. Sci. USA **96,** 3292–3297.

Feys, B.J., Moisan, L.J., Newman, M.A., and Parker, J.E. (2001). Direct interaction between the Arabidopsis disease resistance signaling proteins, EDS1 and PAD4. EMBO J. **20,** 5400–5411.

He, Y.H., and Gan, S.S. (2002). A gene encoding an acyl hydrolase is involved in leaf senescence in Arabidopsis. Plant Cell **14,** 805–815.

Jirage, D., Tootle, T.L., Reuber, T.L., Frost, L.N., Feys, B.J., Parker, J.E., Ausubel, F.M., and Glazebrook, J. (1999). *Arabidopsis thaliana PAD4* encodes a lipase-like gene that is important for salicylic acid signaling. Proc. Natl. Acad. Sci. USA **96,** 13583–13588.

Karpova, T.S., Baumann, C.T., He, L., Wu, X., Grammer, A., Lipsky, P., Hager, G.L., and McNally, J.G. (2003). Fluorescence resonance energy transfer from cyan to yellow fluorescent protein detected by acceptor photobleaching using confocal microscopy and a single laser. J. Microsc. **209,** 56–70.

Kinkema, M., Fan, W.H., and Dong, X.N. (2000). Nuclear localization of NPR1 is required for activation of *PR* gene expression. Plant Cell **12,** 2339–2350.

Llompart, B., Castells, E., Rio, A., Roca, R., Ferrando, A., Stiefel, V., Nech, P.P., and Casacuberta, J.M. (2003). The direct activation of MIK, a germinal center kinase (GCK)-like kinase, by MARK, a maize atypical receptor kinase, suggests a new mechanism for signaling through kinase-dead receptors. J. Biol. Chem. **278,** 48105–48111.

Lu, W.G., Yamamoto, V., Ortega, B., and Baltimore, D. (2004). Mammalian Ryk is a Wnt coreceptor required for stimulation of neurite outgrowth. Cell **119,** 97–108.

Mateo, A., Muhlenbock, P., Rustérucci, C., Chang, C.C., Miszalski, Z., Karpinska, B., Parker, J.E., Mullineaux, P.M., and Karpinski, S. (2004). *LESION SIMULATING DISEASE 1* is required for acclimation to conditions that promote excess excitation energy. Plant Physiol. **136,** 2818–2830.

Mou, Z., Fan, W.H., and Dong, X.N. (2003). Inducers of plant systemic acquired resistance regulate NPR1 function through redox changes. Cell **113,** 935–944.

Park, S.H., Zarrinpar, A., and Lim, W.A. (2003). Rewiring MAP kinase pathways using alternative scaffold assembly mechanisms. Science **299,** 1061–1064.

Petersen, M., et al. (2000). *Arabidopsis* MAP kinase 4 negatively regulates systemic acquired resistance. Cell **103,** 1111–1120.

Rigaut, G., Shevchenko, A., Rutz, B., Wilm, M., Mann, M., and Séraphin, B. (1999). A generic protein purification method for protein complex characterization and proteome exploration. Nat. Biotechnol. **17,** 1030–1032.

Rustérucci, C., Aviv, D.H., Holt, B.F., Dangl, J.L., and Parker, J.E. (2001). The disease resistance signaling components *EDS1* and *PAD4* are essential regulators of the cell death pathway controlled by *LSD1* in Arabidopsis. Plant Cell **13,** 2211–2224.

Shah, H., Gadella, T.W.J., van Erp, H., Hecht, V., and de Vries, S.C. (2001). Subcellular localization and oligomerization of the *Arabidopsis thaliana* somatic embryogenesis receptor kinase 1 protein. J. Mol. Biol. **309,** 641–655.

Shirasu, K., Nielsen, K., Piffanelli, P., Oliver, R., and Schulze-Lefert, P. (1999). Cell-autonomous complementation of *mlo* resistance using a biolistic transient expression system. Plant J. **17,** 293–299.

Tissier, A.F., Marillonnet, S., Klimyuk, V., Patel, K., Torres, M.A., Murphy, G., and Jones, J.D.G. (1999). Multiple independent defective Suppressor-mutator transposon insertions in Arabidopsis: A tool for functional genomics. Plant Cell **11,** 1841–1852.

Wang, W.Y., Hall, A.E., O'Malley, R., and Bleecker, A.B. (2003). Canonical histidine kinase activity of the transmitter domain of the ETR1 ethylene receptor from Arabidopsis is not required for signal transmission. Proc. Natl. Acad. Sci. USA **100,** 352–357.

Witte, C.P., Noël, L.D., Gielbert, J., Parker, J.E., and Romeis, T. (2004). Rapid one-step protein purification from plant material using the eight-amino acid StrepII epitope. Plant Mol. Biol. **55,** 135–147.

Xiao, S., Calis, O., Patrick, E., Zhang, G., Charoenwattana, P., Muskett, P., Parker, J.E., and Turner, J.G. (2005). The atypical resistance gene, *RPW8*, recruits components of basal defence for powdery mildew resistance in Arabidopsis. Plant J. **42,** 95–110.

Xiao, S.Y., Brown, S., Patrick, E., Brearley, C., and Turner, J.G. (2003). Enhanced transcription of the Arabidopsis disease resistance genes *RPW8.1* and *RPW8.2* via a salicylic acid-dependent amplification circuit is required for hypersensitive cell death. Plant Cell **15,** 33–45.

Zhang, Y., and Li, X. (2005). A putative nucleoporin 96 is required for both basal defense and constitutive resistance responses mediated by *suppressor of npr1-1,constitutive 1*. Plant Cell **17,** 1306–1316.

Zhang, Y.L., Goritschnig, S., Dong, X.N., and Li, X. (2003). A gain-of-function mutation in a plant disease resistance gene leads to constitutive activation of downstream signal transduction pathways in *suppressor of npr1-1, constitutive 1*. Plant Cell **15,** 2636–2646.

Zhou, F., Menke, F.L., Yoshioka, K., Moder, W., Shirano, Y., and Klessig, D.F. (2004). High humidity suppresses *ssi4*-mediated cell death and disease resistance upstream of MAP kinase activation, H_2O_2 production and defense gene expression. Plant J. **39,** 920–932.

Zhou, N., Tootle, T.L., Tsui, F., Klessig, D.F., and Glazebrook, J. (1998). *PAD4* functions upstream from salicylic acid to control defense responses in Arabidopsis. Plant Cell **10,** 1021–1030.